Retrofits of a partial combustion lance using a computational fluid dynamics

Woon Phui Law[1], Jolius Gimbun[1,2]
[1]Faculty of Chemical & Natural Resources Engineering,
[2]Centre of Excellence for Advanced Research in Fluid Flow (CARIFF),
Universiti Malaysia Pahang,
26300 Gambang, Pahang, Malaysia
woonphui@gmail.com, jolius@mp.edu.my

***Abstract*—This paper presents a computational fluid dynamics (CFD) simulation of a partial combustion lance (PCL) aiming to evaluate the effect of nozzle design and oxygen flowrate on its performance. At first, the modelling strategy was developed by evaluating the effect of discretization, pressure interpolation scheme and turbulence models on the prediction accuracy. Four turbulence models, namely standard *k-ε* (SKE), realizable *k-ε* (RKE), renormalized (RNG) *k-ε* and Reynolds stress model (RSM) were used. Combustion was modelled using the species transport model, whereas the heat transfer was calculated by considering a combined convection-radiation boundary condition. The best CFD prediction was obtained using the third-order MUSCL (Monotonic for upstream-centred scheme for conservation law), PRESTO (Pressure staggering option) pressure interpolation scheme and RSM, yielding an error of 2.23% from the experimentally measured temperature. The new nozzle design shows increases in excess of 70% of the peak combustion temperature of the PCL. It was found that 40% increase in oxygen flowrate increased the peak combustion temperature of the PCL by about 12%. Dual lance was found to be more effective than the single lance operating at a similar flowrate. The finding obtained from this work may be useful for design retrofits of a PCL.**

Keywords—CFD; modelling strategy; URANS; turbulence; combustion; nozzle design; oxygen lance

I. INTRODUCTION

Partial combustion system is often used in iron making plant to increase the reducing gas temperature and to promote in-situ reforming. Installation of a partial combustion system at the transfer line between the reducing gas heater and the iron reduction reactor is vital to reduce the reforming gas consumption and to increase overall reactor performance due to increase in operating temperature. In most cases, the partial combustion unit suffers from a low combustion efficiency and poor heat transfer due to several factors. The design configuration of the partial combustion lance (PCL) is one of the major factors contributing to these issues. For instance, low oxygen concentration in combustion air gives a slower combustion rate and smaller flame. This results in insufficiently high flame temperature and increased pollutant emission [1]. Therefore, poor PCL designs can significantly affect performance of combustion.

Fluid flow in a PCL had been widely studied experimentally and numerically by many researchers [2-5]. Cheaper measurement technique may be performed using a hot-wire anemometry [6]. Of course, advanced techniques such as particle image velocimetry (PIV), can provide more detail visualizations on the flow pattern [7]. However, experimental measurement using PIV is costly and has an inherent limitation. PIV measurement relying on the CCD camera for image capturing hence it is not applicable on an opaque wall beside it is potentially dangerous to employ a PIV measurement for a large industrial-scale PCL operating at a temperature above 1000 K. Since partial combustion involves complex phenomena, including simultaneous chemical reactions, turbulent mixing and heat transfer, it is not appropriate to perform the evaluation experimentally. Thus, a CFD technique which can provide comprehensive information on the fluid flow, reaction, heat and mass transfer in the PCL was employed in this work.

Most of the previous work used *k-ε* based models [3, 8, 9, 10], (i.e., standard *k-ε* (SKE), realizable *k-ε* (RKE) and renormalized (RNG) *k-ε*). The reason is mainly due to the robustness of SKE, which converges easily and has a relatively low computational demand. Thus, most of the previous work employed the SKE approach without any comparison between different turbulence models. So far, very limited study on the effect of the modelling strategy, (i.e., discretization, pressure interpolation scheme and turbulence models) on the prediction accuracy for PCLs has been performed. Furthermore, some numerical studies did not perform a validation with experimental data [11]. A well-developed numerical model for PCL is important because they can significantly affect the accuracy and reliability of CFD studies. Hence, this work aims to develop a modelling strategy to predict the temperature profile in a PCL. The modelling strategy was developed by performing a grid dependency analysis, evaluating the effects of discretization, pressure interpolation schemes and turbulence models. The CFD prediction was compared with the experimentally measured temperature. Once validated, the model was used to study the

MyMaster Scholarship by Ministry of Education Malaysia.
Funding (GRS140331) by Universiti Malaysia Pahang.

effect of nozzle design and oxygen flowrate on the temperature profile in the PCL.

II. CFD APPROACH

A. Geometry and Computational Grid

A three-dimensional horizontal cylindrical PCL fitted with two oxygen lances and nozzles, as shown in Fig. 1, was prepared using GAMBIT 2.4.6. The cylindrical PCL is 6.35 m in length and has a diameter of 1.266 m. Each oxygen lance has a length of 0.483 m and a diameter of 0.06 m while the nozzle has a length of 0.03 m and a diameter of 0.022 m. Both oxygen lances are installed 1.35 m from the PCL inlet. The distance between both oxygen lances is 0.30 m. Nozzles are attached 0.039 m from the lances. The fuel gas is injected into PCL at 1203 K and 118 m/s, while pure oxygen is injected at 300 K and at 70 m/s through the nozzles. The PCL wall is made of 0.03 m thick steel with a convective heat transfer coefficient of 0.5 W/m^2·K. The geometry of the PCL in this work is similar to the one studied by Zain, Gimbun & Hassan [12]. The geometry in this work was meshed using unstructured meshes, i.e., tetrahedral and hexahedral meshes, which were then converted into a polyhedra mesh, as shown in Fig. 2. Higher grid densities (finer cells) were created near the oxygen lances and flame region, while the rest of the PCL regions were meshed with coarser cells.

The original nozzle design is wingless, which leads to a poor turbulent mixing and a low flame intensity, thus, modification of the nozzle design was studied. Three new nozzle designs were proposed for evaluation. The influence of new nozzle designs on the performance of the PCL was evaluated. A sketch of the original and three new nozzle designs is shown in Fig. 1. The cross-sectional areas of the nozzle wings were set constant for all designs to provide a fair comparison.

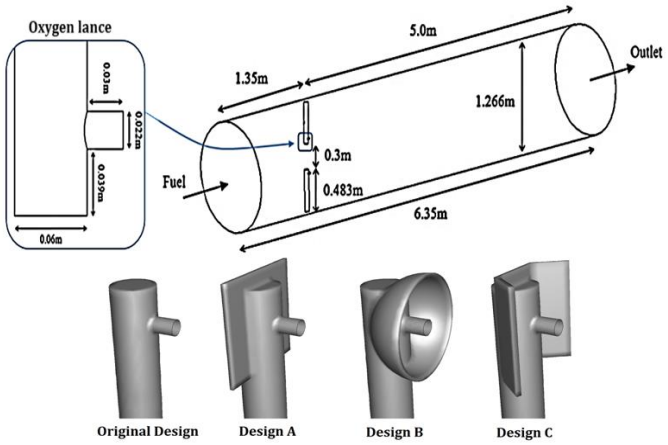

Fig. 1. A schematic of PCL and oxygen lance geometry.

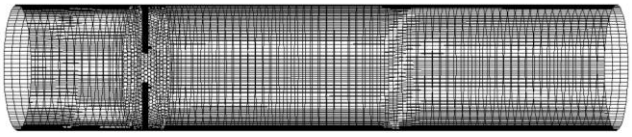

Fig. 2. Surface mesh of PCL.

B. Turbulence Modelling

Selection of the turbulence model is very important in CFD simulation to obtain a good prediction. In this work, three turbulence models (i.e., SKE, RKE and RNG *k*-*ε*) was employed. Two-equation SKE is the most-used turbulence model owing to its simplicity, robustness and has a relatively low computational demand. As the shortcoming of SKE is known, an effort was made to introduce a turbulence model that takes into account the swirling effect as well as to ensure a realistic value (non-negative) for C_μ in *k*-equation [13]. Unlike the SKE, C_μ coefficient in RKE is not constant and computed as a function of local states of the flow to ensure normal stresses are positive under all flow conditions. Therefore, this model can provide a better prediction on rotation and separation flows [14].

RNG *k*-*ε* was derived from renormalized group theory by Yakhot and Orzag [15]. In RNG *k*-*ε*, the small-scale eddies are eliminated, and the transport coefficient is renormalized. RNG differs from standard *k*-*ε* because it has an additional term to account for swirl effect, has an analytical equation for turbulent Prandtl number (Pr_t) and additional term (R_ε) in ε transport equation to account for the interaction between turbulence dissipation and mean shear. This additional term gives a slight reduction of dissipation rate, as the result reduces the effective viscosity. Thereby, RNG *k*-*ε* model can provide better prediction for a region with large strain rate and streamline curvature [15].

RSM solves one equation for each Reynolds stresses and thus the first-order turbulence modelling is not required, eliminating the isotropic eddy viscosity assumption. RSM solves transport equations for Reynolds stresses and dissipation rate [16]. This model accounts for the effects of streamline curvature, swirl, rotation and rapid changes in strain rate in a more rigorous manner compared to the one-equation and two-equation models, hence RSM has potential to give accurate predictions for complex flows [14]. Modelling using RSM requires a relatively higher computing cost to solve the seven additional transport equations.

C. Heat Transfer Modelling

In the PCL, both convective and radiative heat transfer occurs simultaneously [17]. According to Abbasi Khazaei, Hamidi & Rahimi [11], radiation is a dominant heat transfer, which accounts for 96% of total heat transfer while only 4% is a convective heat transfer. The convective heat transfer equation is given by;

$$\frac{\partial}{\partial t}(\rho E)+\frac{\partial}{\partial x_i}[u_i(\rho E+P)=\frac{\partial}{\partial x_j}\left[k_{eff}\frac{\partial \tau}{\partial x_j}+u_i(\tau_{ij})_{eff}\right]+S_h \quad (1)$$

where E is total energy, P is pressure, k_{eff} is the effective thermal conductivity, S_h is source term and $(\tau_{ij})_{eff}$ is a deviatoric stress tensor. The radiative heat transfer equation [18] is given by;

$$\alpha_m\frac{\partial \overline{I_m}}{\partial x}+\beta_m\frac{\partial \overline{I_m}}{\partial y}+\gamma_m\frac{\partial \overline{I_m}}{\partial z}+\overline{\kappa I_m}=\overline{\kappa I_b} \quad (2)$$

where I_m is radiation intensity, α_m, β_m, γ_m is direction cosines along the coordinate, κ is absorption coefficient and I_b is black body intensity.

D. Species Transport Modelling

PCL mainly involves species transport (including reaction) and turbulent mixing. Interaction between fuel gas and oxygen affects the flame pattern and reaction intensity, hence may affect the overall performance of a PCL. The chemical reactions during partial combustion in the PCL are shown by;

$$CH_4+2O_2\rightarrow CO_2+2H_2O \quad (3)$$

$$CH_4+1.5O_2\rightarrow CO+2H_2O \quad (4)$$

$$CO+0.5O_2\rightarrow CO_2 \quad (5)$$

$$H_2+0.5O_2\rightarrow H_2O \quad (6)$$

$$CO_2\rightarrow CO+0.5O_2 \quad (7)$$

All of the reactions involved are exothermic, except for the carbon dioxide (CO_2) dissociation in Equation (7). The composition of the inlet gases is given in Table I. In this work, partial combustion of syngas was calculated by the combination of finite rate and eddy dissipation model (EDM) which is available in species transport module in Fluent Ansys. The finite rate model calculates the chemical reaction rate according to the Arrhenius equation where the turbulent mixing effect is negligible. In EDM, a fast chemical reaction was assumed to be controlled by turbulent mixing. A finite rate-EDM approach includes both Arrhenius and mixing rate, whereby the lower rate from either model dictates the reaction.

E. Modelling Strategy

In this work, simulation was performed using a HP Z220 workstation with Quadcore Xeon E3-1225 processor (3.2 GHz) and 8GB of RAM. The CFD simulation was initiated by assuming a uniform (70 m/s) x-velocity inside the whole domain (patched) to facilitate faster convergence, knowing the inlet velocity in the x-direction of 118 m/s. At first, the PCL simulation was performed using a first-order discretization. The physical properties of air (i.e., density, specific heat, thermal conductivity and viscosity) from 300K to 3500K was introduced to the simulation as a piecewise linear function. A higher-order discretization (i.e., second-order, QUICK (Quadratic upwind interpolation for convective kinematic) and third-order MUSCL (Monotonic for upstream-centred scheme for conservation law)) was enabled later to obtain an accurate prediction. The simulation was performed using the unsteady solver, and all residuals were set to fall below 1×10^{-4} to ensure a good convergence was achieved. Data were recorded for over 1000 time steps and were averaged once a pseudo-steady condition was reached.

TABLE I. COMPOSITION OF INLET GASES

Component	Mass Fraction
CH_4	0.132
CO	0.486
CO_2	0.072
H_2	0.154
H_2O	0.029
N_2	0.126

TABLE II. GRID DEPENDENT STUDY

Case	Temperature (K)	Error (%)	CPU Time (s/iteration)
Experiment	1293.0	-	-
Coarse Grid	1194.5	7.62	< 0.90
Intermediate Grid	1222.6	5.44	1.80
Fine Grid	1240.6	4.05	2.71

III. RESULT AND DISCUSSION

A. Grid Dependency Analysis

The geometry in this work was meshed using unstructured meshes, i.e., tetrahedral and hexahedral meshes, which were then converted into a polyhedra mesh. Three different grid densities of PCL, denoted as coarse (149k nodes), intermediate (418k nodes) and fine grids (694k nodes). A steady-state, standard pressure interpolation scheme and SKE turbulence model were employed. Prediction obtained from the three different grids is shown in Table II and compared with the experimental data [12]. Zain, Gimbun & Hassan [12] reported an experimentally measured temperature of 1293 K, at position 5.85 m from the inlet and approximately 0.373 m from PCL wall. The CPU time for the coarse grid is below 0.9 second/iteration, whereas the intermediate and fine grid needs 1.8 and 2.7 s/iteration, respectively. Among these grids, prediction using the coarse grid yielded the largest error (7.62%). A notable improvement in the prediction accuracy obtained using the intermediate (5.44%) and fine (4.05%) grids were observed. The intermediate grid was selected for the rest of this work to minimise the computational effort, since prediction by the fine and intermediate grid is not substantially different.

B. Discretization

The effect of the discretization scheme on the CFD prediction was studied using a steady-state simulation, standard pressure interpolation scheme and SKE turbulence model. Four discretization methods, namely, the first-order

upwind, second-order upwind, third-order MUSCL and QUICK schemes were compared. The comparison of the temperature predictions obtained using different numerical discretization methods with the experimental measurement [12] is shown in Fig. 3. The fastest convergence was achieved using the first-order upwind scheme. Nonetheless, the prediction is less accurate (7.46%) compared to higher-order schemes. This can be ascribed to the susceptibility of the first-order scheme to the numerical diffusion. The higher-order schemes (i.e., second order, QUICK and MUSCL) yielded a better prediction with error ranging from 5.31 to 5.81%. The best agreement with the experimentally measured temperature was obtained using the third-order MUSCL scheme. The QUICK scheme worked as a third-order scheme in the structured hexahedral mesh, but acted as a second-order scheme in unstructured mesh like the one used in this work.

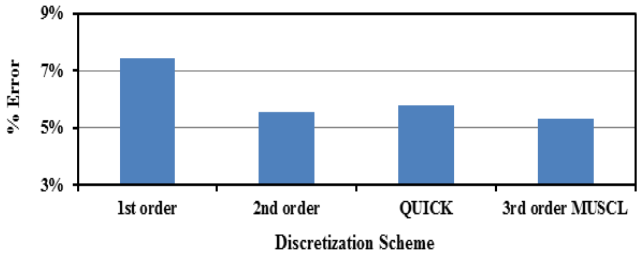

Fig. 3. Comparison of discretization scheme.

Hence, only moderate accuracy was achieved. On the contrary, the third-order MUSCL is applicable to all types of meshes and hence used for the rest of this work.

C. Pressure Interpolation Scheme

The effect of various pressure interpolation schemes, namely, standard, second-order, linear and PRESTO (Pressure staggering option), were studied using a steady-state simulation, the third-order MUSCL scheme and an SKE model. The CFD prediction of the static temperature is compared with the experimental data [12] as shown in Fig. 4. The differences in the prediction accuracy of these four schemes are not noteworthy. It is known that prediction using the linear pressure scheme is less accurate than the second-order pressure scheme [16]; the same was also observed in this study. The result from the PRESTO scheme showed some fluctuation, although the mean error was the lowest (4.88%). In contrast, all other schemes have an error of more than 5%. This work indicates that the PRESTO scheme is more suitable for fluid flow modelling in a PCL.

D. Turbulence Model

Fig. 5 shows prediction errors of static temperature in PCL obtained using a different turbulence models, namely, SKE, RKE, RNG and RSM. The result clearly showed that RSM produced the lowest error (2.23%) compared to other turbulence models. This may be attributed to a comprehensive turbulence modelling in RSM which abandon the assumption of isotropic turbulence, unlike in the *k-ε* based models. Turbulent flow is anisotropic in nature, and hence RSM is well suited for turbulence modelling [16, 19]. In contrast, SKE, RKE and RNG give a reasonable prediction with error of than 4.00% error due to the isotropic eddy viscosity assumption. This finding suggests that RSM has ability to predict accurately the turbulence flow in PCL.

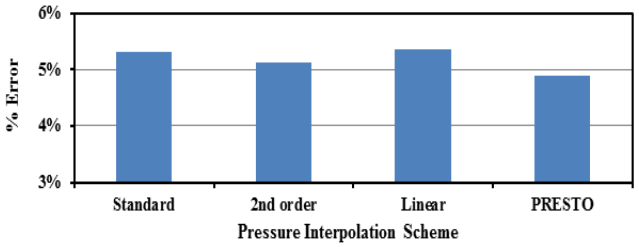

Fig. 4. Comparison of pressure interpolation scheme.

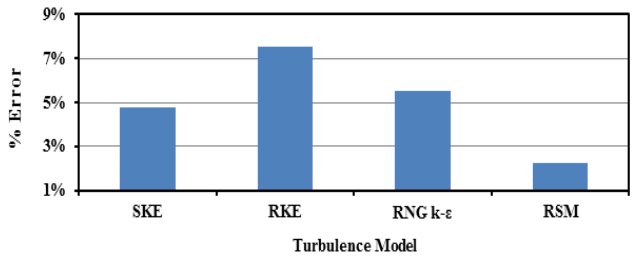

Fig. 5. Comparison of turbulence model.

E. Effect of Nozzle Design

The effect of the wing addition prior to the oxygen nozzle was studied by evaluating three different wing designs of a roughly similar cross-sectional area. The temperature profile was predicted along the radial position after the nozzle, 1.5 m from the PCL inlet, as shown in Fig. 6. The chemical reaction between the fuel and oxygen takes place in the upwind region of the nozzle. Hence, peak temperature was achieved at two regions (-0.3 m < Z < -0.1 m and 0.1 m < Z < 0.3 m) and decreased towards the PCL wall, as shown in Figs. 6 and 7. This region is known as the combustion region. The result indicated that the new nozzle design gave a better combustion performance (i.e., higher peak temperature and bigger flame) compared to the original design. Among the new designs, design A showed the best performance, providing the highest maximum temperature (over 70% higher than the original design). This is due to the recirculation and enhanced mixing of the methane and oxygen induced by the wing structure.

The attached wing is designed to facilitate the turbulence-induced mixing between the syngas and oxygen, thereby increasing the reaction rates of the combustion processes. Design A produced the highest turbulent kinetic energy, whereas the wingless design in the original PCL design showed a lower turbulent kinetic energy, as shown in Fig. 8. In fact, all of the proposed winged nozzle designs had a much higher turbulent kinetic energy compared to the original design due to the disturbance of the flow by the wings. Design A has a 90° angle to the direction of the flow and hence produced the most turbulence. In contrast, design B and C have a curved edge facing the direction of the flow, resulting in less intense turbulence.

Fig. 9 shows the contour plots for five chemical reactions in the PCL. Reactions 1 and 4 show the partial and complete combustion of methane (CH_4); reactions 2 and 3 are the partial combustion of syngas, and reaction 5 represents CO_2 dissociation. Other than reaction 5, all of the reactions in this work are exothermic. Syngas, which is composed of carbon monoxide (CO) and hydrogen (H_2), has much higher reaction rates than that of methane, as shown in Fig. 9. The lower reaction intensity of CH_4 may also be attributed to the its lower proportion in the inlet gas (13.2%). Incomplete and high-temperature reactions lead to favourable conditions for CO formation. It is understood that CO_2 dissociation into CO and O_2 increases with temperature, especially above 1800 K [20]. This explained the higher rates of reaction 5 in this work with the modified nozzle design, which lead to significantly higher temperatures than the original design (Fig. 7). Combustion in a PCL is affected by turbulent mixing between the inlet gas and oxygen from the nozzle. Greater turbulent mixing between the species induces intense chemical reactions, resulting in a higher flame intensity. The highest peak combustion temperature and largest flame were achieved by adding a flat wing (design A) to the original design.

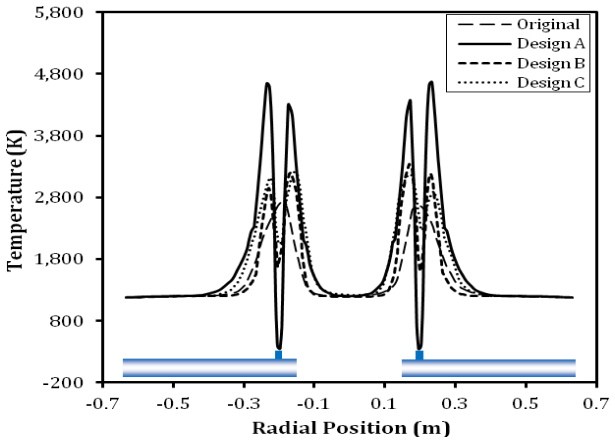

Fig. 6. Predicted mean temperature profile for four nozzle designs at 1.5 m.

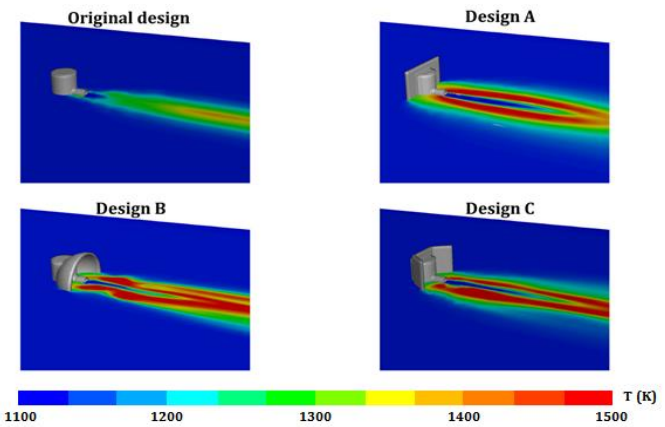

Fig. 7. Time-averaged static temperature contour plot for four nozzle designs.

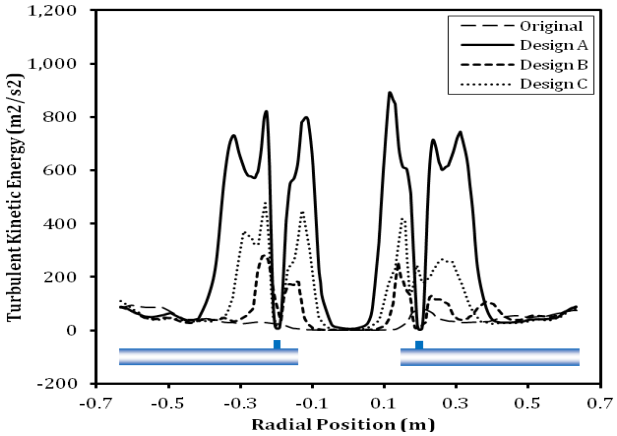

Fig. 8. Turbulent kinetic energy prediction for four nozzle designs.

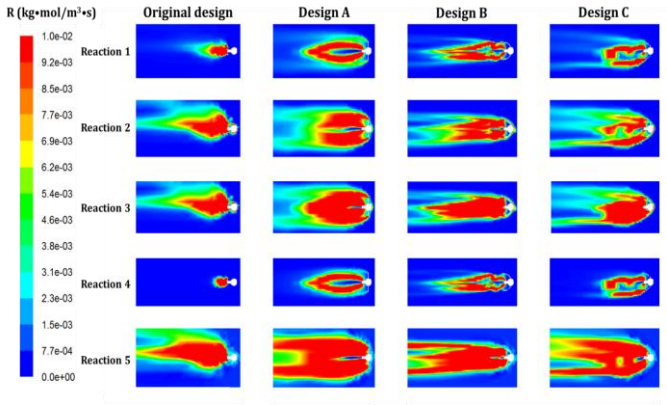

Fig. 9. Instantaneous reaction rates contour plot for four nozzle designs.

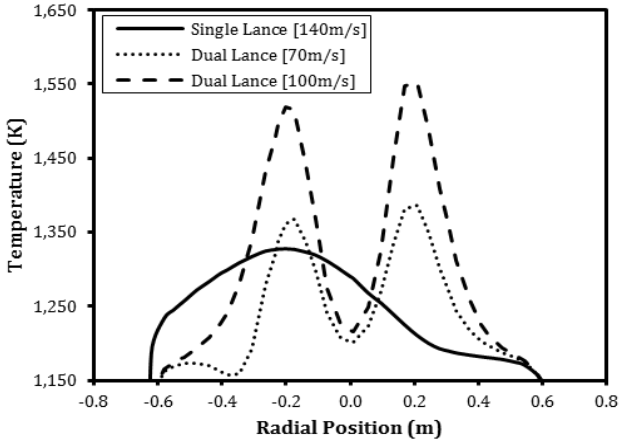

Fig. 10. Predicted mean temperature profile for different oxygen flowrate.

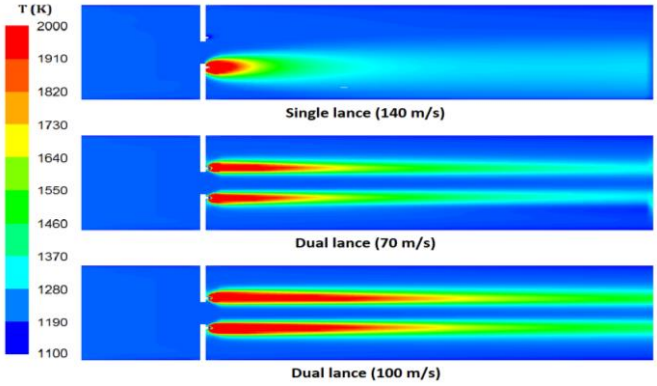

Fig. 11. Temperature contour plot for different oxygen flowrate.

F. Effect of Oxygen Flowrate

The influence of the oxygen flowrate on the combustion temperature was studied by evaluating two different cases, i.e., dual lances operating at different flowrate; and single and dual lances operating at a same total flowrate. The predicted temperature profile along the radial position at 5.85 m from PCL inlet is shown in Fig. 10. The dual temperature peak was observed at two regions (-0.3 m < Y < -0.1 m and 0.1 m < Y < 0.3 m) when dual lance is used. Whereas only a single temperature peak at -0.3 m < Y < -0.1 m was observed in the single lance operation. Higher oxygen flowrate enhanced the combustion reaction. This resulted in larger flame and higher temperature as shown in Fig. 11. Thereby, increasing the oxygen flowrate from 70 m/s to 100 m/s in dual lance operation increased the peak temperature from 1386 K to 1553 K (12% increased). The second case evaluates the effect of single and dual lance operating at a same total flowrate. The two lances have a same surface area, in a way that the oxygen flowrate is proportional to the inlet velocity. The dual lance was set to operate at 70 m/s in each lance while the single lance was set to operate at 140 m/s to ensure a similar flowrate can be obtained. A single lance produced higher temperature and wider flame in the combustion zone (Fig. 11). However, the combustion rate decreased towards the PCL outlet due to high consumption of fuel at the combustion zone. Therefore, the peak temperature achieved from a single lance (1328 K) is lower than the dual lance (1386 K).

IV. CONCLUSIONS

A CFD modelling strategy was successfully developed for a PCL. The best prediction was obtained using a combination of a third-order MUSCL, PRESTO pressure interpolation scheme and RSM, with an error of 2.23% from the measured combustion temperature. The new nozzle design showed a significant improvement in the PCL combustion, with a peak temperature over 70% higher than the original design. The highest peak combustion temperature was achieved by attaching a flat wing (Design A) compared to the original wingless oxygen nozzle design. It was found that a 40% increase in the oxygen flowrate yielded a 12% increased of combustion temperature. This work also indicated that dual lance provides a better combustion performance than the single lance working at same total oxygen flowrate. The CFD model in this work may serve as an useful tool to evaluate the design of PCLs or for design retrofitting of an existing PCL.

Acknowledgment

W.P. Law thanks Ministry of Education Malaysia for the MyMaster scholarship. The authors acknowledge funding from Universiti Malaysia Pahang through GRS140331.

References

[1] Y. Saso, H. Gotoda, and Y. Ogawa, "Effect of oxygen concentration on the carbon monoxide yields from methane and methanol flames," Fire Safety Science-Proceedings of the Eight International Symposium, International Association for Fire Safety Science, pp. 1013-1022, 2005.

[2] G. Li, H. Zhou, X. Qian, and K. Cen, "Determination of hydrogen production from rich filtration combustion with detailed kinetics based CFD method," Chin. J. Chem. Eng., vol. 16, no. 2, pp. 292-298, 2008.

[3] H. Amirshaghaghi, A. Zamaniyan, H. Ebrahimi, and M. Zarkesh, "Numerical simulation of methane partial oxidation in the burner and combustion chamber of autothermal reformer," Appl. Math. Modell., vol. 34, pp. 2312-2322, 2010.

[4] X. Zhou, C. Chen, and F. Wang, "Modeling of non-catalytic partial oxidation of natural gas under conditions found in industrial reformers," Chem. Eng. Process., vol. 49, pp. 59-64, 2010.

[5] W. Guo, Y. Wu, L. Dong, C. Chen, and F. Wang, "Simulation of non-catalytic partial oxidation and scale-up of natural gas reformer," Fuel Process. Technol., vol. 98, pp. 45-50, 2012.

[6] D. Bradley, and G.F. Hundy, "Burning velocities of methane-air mixtures using hot-wire anemometers in closed-vessel explosions," Symp. (Int.) Combust., vol. 13, no. 1, pp. 575-583, 1971.

[7] Y.W. Zhang, Y. Bo, Y.C. Wu, X.C. Wu, Z.Y. Huang, J.H. Zhou, and K.F. Cen, "Flow behavior of high-temperature flue gas in the heat transfer chamber of a pilot-scale coal-water slurry combustion furnace," Particuology, in press.

[8] D. You, F. Ham, and P. Moin, "Large-eddy simulation analysis of turbulent combustion in a gas turbine engine combustor," Annual Research Briefs, Center for Turbulence Research, pp. 219-230, 2008.

[9] G. Hassan, M. Pourkashanian, D. Ingham, L. Ma, and S. Taylor, "Reduction in pollutants emissions from domestic boilers-computational fluid dynamics study," J. Therm. Sci. Eng. Appl., vol. 1, pp. 1-9, 2009.

[10] C. Galletti, A. Parente, and L. Tognotti, "Numerical and experimental investigation of a mild combustion burner," Combust. Flame, vol. 151, no. 4, pp. 649-664, 2007.

[11] K. Abbasi Khazaei, A.A. Hamidi, and M. Rahimi, "CFD modeling study of high temperature and low oxygen content exhaust gases combustion furnace," Iran. J. Chem. Chem. Eng., vol. 29, no. 2, pp. 85-104, 2010.

[12] M.I.S. Zain, J. Gimbun, and Z. Hassan, "CFD study on the performance of oxygen lance for partial combustion unit at direct reduction plant," International Conference on Chemical Innovation 2011 (ICCI2011), ITC-TATIUC, Teluk Kalong, Terengganu, Malaysia, 23-24 May 2011, unpublished.

[13] T.H. Shih, W.W. Liou, A. Shabbir, Z. Yang, and J. Zhu, "A new k-ε eddy viscosity model for high Reynolds number turbulent flows: Model development and validation," NASA technical memorandum 106721, ICOMP-94-21, CMOTT-94-6, Lewis Research Center, Cleveland, Ohio, 1994.

[14] B. Andersson, R. Andersson, L. Hakansson, M. Mortensen, R. Sudiyo, and B.V. Wachem, Computational Fluid Dynamics for Engineers, New York: Cambridge University Press, 2012.

[15] V. Yakhot, and S.A. Orszag, "Renormalization group analysis of turbulence. I. Basic theory," J. Sci. Comput., vol. 1, no. 1, pp. 3-51, 1986.

[16] Fluent Inc, Fluent 6.3 User's Guide, NH: Lebanon, 2006.

[17] J.R. Welty, C.E. Wicks, R.E. Wilson, and G. Rorrer, Fundamentals of Momentum, Heat, and Mass Transfer, 4th ed., New York: John Wiley & Sons, 2001.

[18] S.C. Paul, and M.M. Paul, "Radiative heat transfer during turbulent combustion process," Int. Commun. Heat Mass Transfer, vol. 37, pp. 1-6, 2010.

[19] J. Gimbun, "CFD simulation of aerocyclone hydrodynamics and performance at extreme temperature," Eng. Appl. Comput. Fluid Mech., vol. 2, no. 1, pp. 22-29, 2008.

[20] Y. Nigara, and B. Cales, "Production of carbon dioxide by direct thermal splitting of carbon dioxide at high temperature," Bull. Chem. Soc. Jpn., vol. 59, pp. 1997-2002, 1986.